J Mater Sci

Composites & nanocomposites

Interfacial interaction-induced temperature-dependent mechanical property of graphene-PDMS nanocomposite

Xin Wang[1], Zhekun Shi[1], Fandong Meng[1], Yan Zhao[1], Zhongshuai Wu[2], Yifeng Lei[1], and Longjian Xue[1,*]

[1] *School of Power and Mechanical Engineering & The Institute of Technological Science, Wuhan University, South Donghu Road 8, 430072 Wuhan, China*

[2] *Dalian National Laboratory for Clean Energy, Dalian Institute of Chemical Physics, Chinese Academy of Sciences, 457 Zhongshan Road, Dalian 116023, China*

Received: 12 July 2019
Accepted: 11 October 2019

ABSTRACT

Polydimethylsiloxane (PDMS) and graphene-PDMS nanocomposites (GP) have been widely studied because of their excellent properties, of which the elastic modulus is very important for various applications. Here, the dependence of the elastic modulus of properly cured PDMS and GP on the temperature has been investigated. For both PDMS and GP, a critical temperature (T_c) has been found, which originates from the strong affinity of PDMS chains to the PDMS network and graphene sheet, as suggested by molecular dynamics simulation. Graphene inhibits the cross-linking of PDMS close to its surface, which leads to the reduced elastic modulus of GP (E_{GP}). Only when the temperature is above T_c, E_{GP} increases with temperature. This is the result of the entropy elasticity of PDMS and the re-initiated cross-linking of PDMS. However, the elastic moduli of PDMS and GP are independent of the temperature below T_c. Here, the study provides a guideline for the preparation and using of PDMS and its composite at various temperatures.

Introduction

Composite material has drawn considerable attention to the fundamental research also in a wide range of applications as it possesses superior properties in comparison with the simple combination of its constitutive components. For instance, the graphene-PDMS nanocomposite (GP) has been potentially used in flexible and smart devices, e.g. sensors/actuators, soft robots, and so on [1–5]. The polydimethylsiloxane (PDMS) offers high flexibility, good biocompatibility and high optical transparency, while graphene offers good conductivities of heat and electricity,

Xin Wang and Zhekun Shi have contributed equally to this work.

Address correspondence to E-mail: xuelongjian@whu.edu.cn

https://doi.org/10.1007/s10853-019-04126-y

Published online: 01 November 2019

large elastic modulus [5–8]. In the case of composite, along with the inherent properties of matrix and fillers, the interface between the matrix and the fillers also plays an active role in determining the properties of the composite.

It has been widely demonstrated that a proper interaction between polymer matrix and fillers leads to a significant enhancement of the mechanical properties in composites [9–13]. Due to the van der Waals adhesion between PDMS and graphene, PDMS close to the surface of graphene tends to align along the lattice of graphene, forming an interphase layer of physical cross-linking [10, 11]. This effect became stronger when PDMS was mixed with graphene oxide (GO) [11]. GO causes strong hydrogen-bond interactions between PDMS chains and GO, leading to the formation of an even thicker interphase layer [10]. Therefore, the physical cross-linking inhibits the chemical cross-linking of PDMS. It has also been proposed that the entanglement of polymer chains on nanofillers may be responsible for the reduction in chemical cross-linking [14]. On the other hand, the addition of additives having large elastic modulus will definitely improve the apparent elastic modulus of the composite with respect to its building matrix [7]. The functionalization of nano-additives with reactive groups could chemically bond nanofillers to the PDMS matrix [12], which can effectively increase the elastic modulus and has been demonstrated to be beneficial for the stress transmission. All of these studies point to the competition between chemical and physical interactions at the PDMS–graphene interface, which would determine or regulate the mechanical properties of GP and its applications.

The using conditions also affect the mechanical properties of GP. For instance, it was demonstrated that the long-term cyclic compression initiated the realignment of PDMS chains along the graphene/GO surface, resulted in a self-stiffening effect [11]. It was argued that this process is a physical, rather than a chemical, phenomenon, even under an elevated temperature (up to 95 °C) [11]. PDMS composites with graphene, GO or carbon nanotubes (CNT) will be heated up through electric current or photo-irradiation in terms of resistance heating or photothermal effect of the additive, which has been intensively involved in the design of sensor/actuator and soft robots [1, 2, 15, 16]. It is worth mentioning that the maximum temperature of a graphene/CNT composite could reach up to ~ 200 °C under the UV irradiation [15]. So, it is curious how will the thermal effects (direct heating, galvanothermy and photothermal, etc.) of GP affect the mechanical property during applications?

Here, the thermal effect on the elastic modulus (E) of properly cured GP (E_{GP}) has been studied. A critical temperature (T_c) has been detected in the temperature sweep of E_{GP} under dynamic thermo-mechanical analysis (DMA) test. Above T_c, E_{GP} was increased rapidly with an increase in temperature, while E_{GP} was invariant of temperature below T_c. The stronger affinity of unreacted dangling chains to graphene than to PDMS network inhibits the cross-linking of PDMS close to the graphene surface. The elevation of temperature above T_c could reinitiate the cross-linking of PDMS, contributing to the increase in E_{GP}. Moreover, it was found the entropy elasticity of PDMS only exists at temperature above T_c. The re-initiated cross-linking and entropy elasticity of PDMS contributed together to the increase in E_{GP} at temperature above T_c. The study provides an in-depth understanding of functioning of graphene/PDMS composite, and also provides the guidelines for the processing and usage of PDMS-based materials at various temperatures.

Materials and methods

Preparation of PDMS and GP samples

PDMS elastomer kit (Sylgard 184) was purchased from Dow Corning (Midland, MI). Graphene was prepared by chemical exfoliation. Two glass slides were separated by a small spacer (1.1 mm) to form a cavity, which served as the mould for samples. The prepolymer and cross-linking agent were mixed in various ratios (5:1, 10:1 and 15:1) to prepare the PDMS precursor. Graphene powder was added to the as-prepared PDMS precursor with concentration ranging from 0.2 to 1.2 wt%. After proper mixing, the PDMS or GP was degassed in a desiccator to remove air bubbles, transferred into a homemade mould by capillary force, and cured at 90 °C for 1 h. After being released from mould, the GP and PDMS samples with thickness of 1.1 mm, length of 40 mm and width of 5 mm were ready for measurements.

Characterization

Morphologies of graphene were examined by atomic force microscopy (AFM, Nano Wizard 4, JPK Inc., Germany) in tapping mode (QI^{TM} mode, scan rate = 1 Hz) and field emission scanning electron microscopy (FE-SEM, ZEISS Sigma, Germany). The Raman spectrum was collected on a RM-1000 confocal Raman microspectroscopy (Renishaw, English) with an Ar^+ laser (λ = 514.5 nm, laser power < 0.4 mW). The dark-field optical microscopy images of GP were captured by Nikon ECLIPSE Ci-L microscope. The storage moduli of GP and PDMS were acquired on a Q800 dynamic thermomechanical analyser (TA Instruments, USA) at a frequency of 1 Hz and amplitude of 15 μm. Elastic moduli of GP and PDMS were determined through uniaxial experiment by a tailored uniaxial/biaxial tensile testing system (IBTC-300, CARE Measurement & Control Co., Ltd.)

Interaction energy calculation

The interaction energy calculations were performed using Amorphous Cell and Forcite simulation modules included in Material Studio. The interface model involving the graphene sheet with 6 × 6 × 1 supercell and the PDMS single chain with six repeated units was created using the Amorphous Cell, followed by a series of energy minimization steps in Forcite to attain a state of minimal potential energy. Subsequently, a series of molecular dynamics simulations with NVT ensemble have been performed for modelling the morphology of the model. The parameters were set as follows: quality was medium, and temperatures were set to 25, 100 and 200 °C. The total simulation time was 1000 ps, and the force-field type was COMPASS II and charges on each atom were generated with the force-field assigned option. Finally, the potential energy was employed to attain the interaction energy of the system at the corresponding temperature. The interface model including PDMS single chain and PDMS network was created and calculated in the same way.

Results and discussion

The use of graphene as nanofiller in a polymer matrix has drawn considerable attention due to the excellent properties of graphene [17, 18]. The graphene sheets were prepared by external chemical exfoliation [19]. The representative Raman spectrum of graphene is shown in Fig. 1a: the D peak at 1357 cm^{-1} is activated in the first-order scattering process of sp^2 carbons by some defects of lattice structure [20], and the *G* peak at 1594 cm^{-1} corresponds to the E_{2g} phonon at the Brillouin zone centre [21]. The intensity ratio between D and G peaks is ~ 0.85, indicating the remaining of a small amount of oxidized points [22]. Graphene sheets had a lateral size of 2–3 micron and a thickness of ~ 1.2 nm, which indicates the graphene sheets have 1 ~ 2 layers (Fig. 1b) [17]. The freestanding graphene sheets show a wrinkled state (Fig. 1c), which is beneficial for a better dispersion of graphene in PDMS matrix and can afford a large strain deformation of resulted GP [6, 23]. 1 wt% graphene sheets were mixed in PDMS precursor (prepolymer to cross-linker is 10:1) and cured at 90 °C for 1 h, resulting in a homogeneous graphene/PDMS nanocomposite (GP) (Fig. 1d).

The influence of temperature on the elastic moduli of GP (E_{GP}) was investigated through DMA test. The E_{GP} was evaluated with respect to the increase in temperature at a rate of increment 3 °C min^{-1} from room temperature (RT) to 250 °C. This temperature range was set according to the decomposition temperature of PDMS [24] and the temperature which GP attains under UV irradiation (250 mW cm^{-2}) (Fig. S1). At room temperature, GP showed an elastic modulus of $E_{GP,RT}$. During the heating process, E_{GP} was kept constant until certain critical temperature ($T_{c,GP}$ = 138.8 ± 1.9 °C) was reached (period I in Fig. 2). After $T_{c,GP}$, E_{GP} was increased quickly at an increasing rate (δ_E) till the set temperature, 250 °C, as designated by period II in Fig. 2. The intersection point of tangent lines of periods I and II defines the temperature T_c. After reaching 250 °C, the sample was naturally cooled down to RT (period III), where the modulus is defined by $E_{GP,RT}'$. Surprisingly, $E_{GP,RT}'$ was twice of $E_{GP,RT}$. However, through the heating process of period IV, at 250 °C, the elastic modulus was also reached in the same value of period III ($E_{GP,250}$). In period IV, the E_{GP} at any intermediate temperature was smaller than that of period III, but much larger than that of the periods of I and II. The further cycles of cooling and heating (C2 and C3) were overlapped with periods III and IV in the first cycle (C1).

The dependence of E_{GP} on temperature was further investigated by varying the concentration of

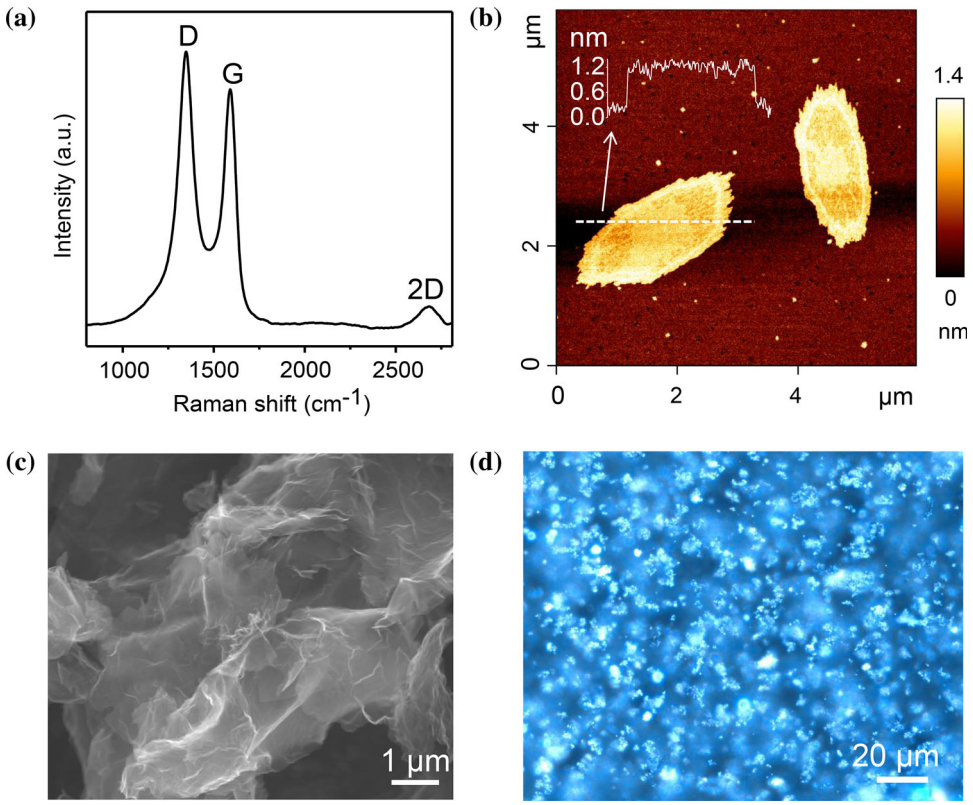

Figure 1 **a** Raman spectrum, **b** AFM, and **c** SEM image of graphene sheets. Inset in **b** shows the height profile of graphene sheet. **d** Optical image of graphene-PDMS composite (GP) under dark-field illumination.

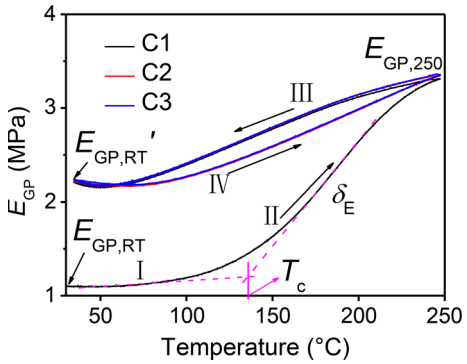

Figure 2 Evolution of elastic modulus of GP (E_{GP}) during representative cycles of heating and cooling (C1–C3). Different periods of heating and cooling (I–IV), elastic modulus at room temperature ($E_{GP,RT}$/$E_{GP,RT}'$) and at 250 °C ($E_{GP,250}$), critical temperature (T_c), and increasing rate of elastic modulus (δ_E) during period II are indicated.

graphene (c_G) in GP and monitoring the heating periods of I and II (Fig. 3). Different from previous reports [6, 7], here we focused on the low c_Gs, mainly smaller than 1 wt%. The prime feature of periods I and II of GP with various graphene concentrations stayed the same that E_{GP} remained constant below the T_c and then increased sharply till the final set temperature (Fig. 3a). From the minute observation of these curves, it was revealed that $E_{GP,RT}$ was slightly increased with the increment of the c_G till 0.4 wt%. The further increment of c_G ($\leq$ 1.2 wt%) caused a sharp decrease in E_{GP} to the value of 0.88 MPa at c_G of 1.2 wt%, which corresponds to a $\sim$ 52.5% decrease in E_{GP} as compared to that of 0.4 wt% GP (Fig. 3b). In the case of $E_{GP,250}$, the same tendency was witnessed, it had the maximum value of 4.18 MPa at c_G of 0.4 wt% where at 1.2 wt%, the value was reduced to $\sim$ 66.7% of it. Similar dependence of apparent elastic modulus on the concentration of additives has also been reported in the composite materials with carbon nanotubes [25], functionalized graphene sheets [26] and Al_2O_3 particles [27], and so on, dispersed in epoxy resins. It was argued that higher concentration may cause the agglomeration of these additives which minimizes the interfacial energy of the composite [28], and as a consequence the apparent elastic modulus is decreased. However, in our case, the increase in c_G from 0.2 to 1.2 wt% does not cause any clear agglomeration of graphene in GP (Fig. S2). Moreover, the initial mixing ratio of prepolymer to cross-linker of PDMS will not influence the dependences of E_{GP} on temperature (Fig. S3). Therefore, it infers that the

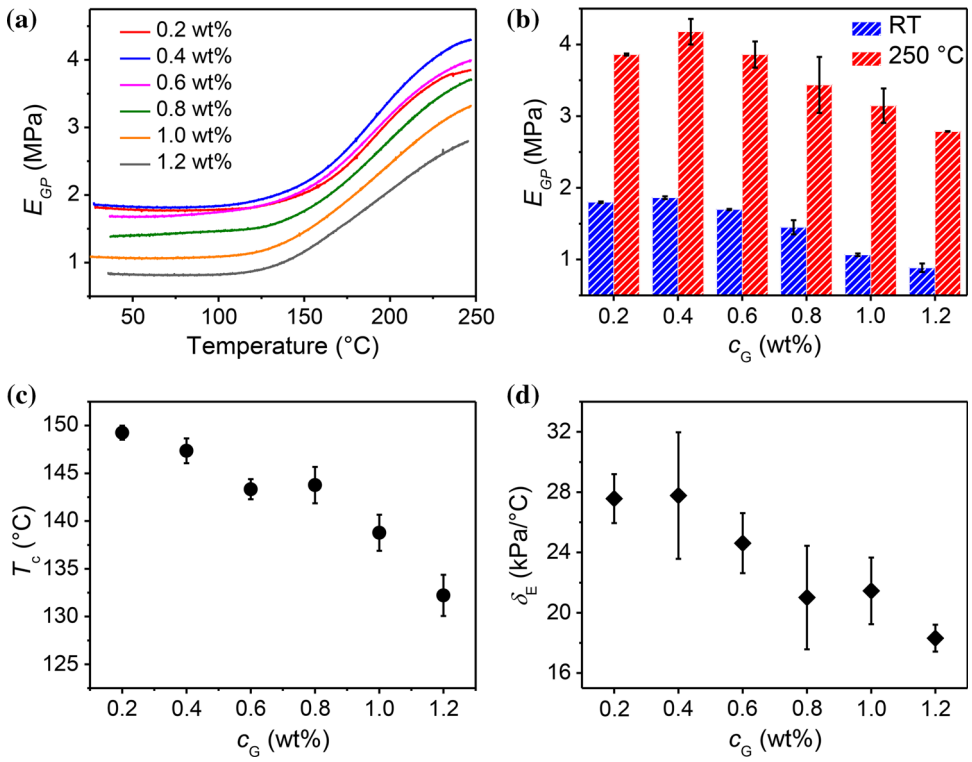

Figure 3 **a** Dependence of elastic modulus of GP (E_{GP}) with various graphene concentrations (c_G) on temperature during the heating process from room temperature to 250 °C. Dependences of **b** E_{GP}s at RT and 250 °C, **c** T_c, and **d** δ_E on the c_G. The data in **b**, **c** and **d** are mean values of three measurements. The error bars indicate standard deviations.

changing of apparent elastic modulus should be the result of competition between inhibited chemical cross-linking of PDMS matrix and the large modulus of graphene.

Furthermore, the T_c was decreased monotonically from 149.3 °C at 0.2 wt% to 132.2 °C at 1.2 wt%, which means a difference of 17.1 °C of T_c was caused by a difference in c_G of only 1 wt% (Fig. 3c). When the temperature was higher than T_c, E_{GP} increased rapidly, showing an increasing speed of δ_E. However, δ_E was decreased from 27.6 kPa °C^{-1} at 0.2 wt% to 18.3 kPa °C^{-1} at 1.2 wt% (Fig. 3d).

In order to understand the temperature dependence of E_{GP}, pure PDMS (prepolymer to cross-linker ratio was 10:1) without graphene sheets was treated in the same way as that of GP. Similar change in elastic modulus of pure PDMS (E_{PDMS}) was observed with an increase/decrease cycles of temperature (Fig. S4a). A critical temperature T_c of 142.8 °C was also witnessed in the heating process of C1 cycle. Extra experiments were also carried out to further confirm the existence of T_c. The PDMS was first cross-linked at 90 °C for 1 h and then further cured for another 2 h at various temperatures (Fig. S4b). The E_{PDMS} of resulted PDMS samples exhibited the same characteristics that E_{PDMS} remained constant till the temperature of 91.2 °C; at higher temperature, it was increased. Though the critical temperature was different from that measured by DMA due to the technical difference of heating process, the extra experiments confirmed the existence of T_c.

Similar dependence of E_{PDMS} on temperature was also found in PDMS with different mixing ratios of prepolymer to cross-linker (Fig. S5). Reducing the amount of cross-linker (for instance, the ratio of prepolymer to cross-linker is 15:1), resulted in a smaller $E_{PDMS,RT}$ and also the corresponding $E_{PDMS,250}$ (Fig. 4a). It is reasonable that a smaller cross-link degree results in a smaller E_{PDMS}. Comparing to GP (1 wt%), E_{PDMS} at RT ($E_{PDMS,RT}$) and E_{250} of PDMS ($E_{PDMS,250}$) were 31% and 17% higher than $E_{GP,RT}$ and $E_{GP,250}$, respectively (Fig. 4b). The followed cooling to RT resulted in a $E_{PDMS,RT}'$ which was also 14% higher. Since the additive graphene has a much larger elastic modulus than PDMS, the reduced $E_{GP,RT}$ and $E_{GP,250}$ should be the result of greatly inhibited chemical cross-linking of the PDMS matrix, which is in good agreement with previous reports [10, 11, 14]. It also suggests that the dependence of E_{GP} on temperature originates from the matrix PDMS, and the additive graphene has an impact on the T_c.

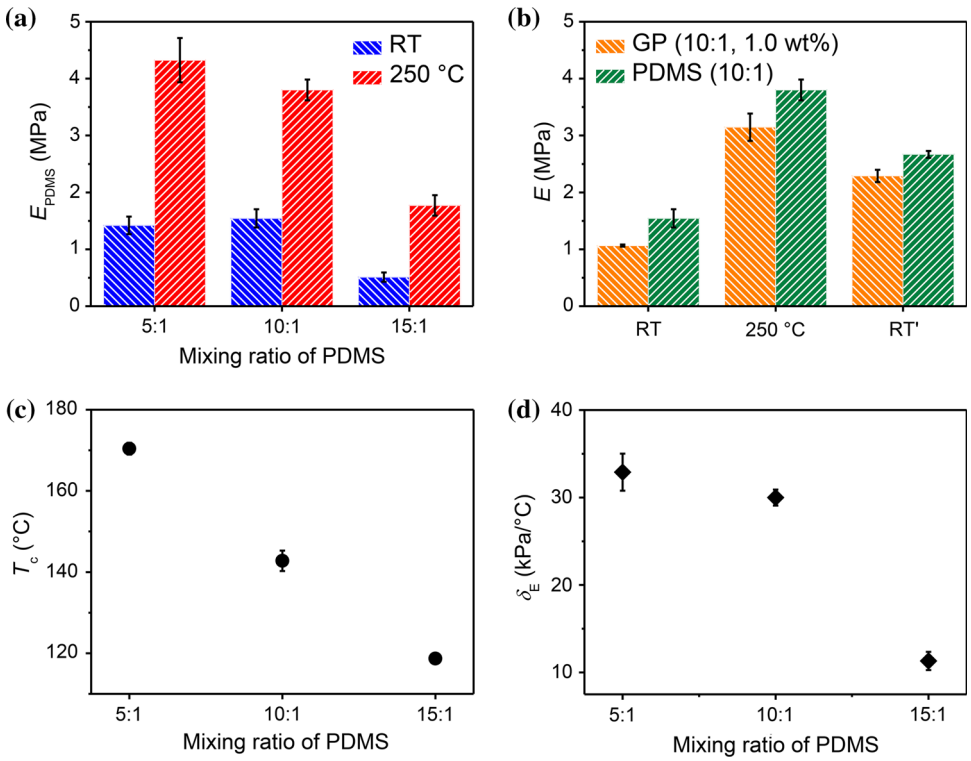

Figure 4 **a** E_{RT} and E_{250} of PDMS with various mixing ratios of precursor to cross-linker of PDMS. **b** E_{GP} (10:1, 1.0 wt%) and E_{PDMS} (10:1) at RT, 250 °C and RT′ (after the heating–cooling process). Dependences of **c** critical temperature (T_c) and **d** increasing rate of elastic modulus (δ_E) on the mixing ratio of PDMS. The data are mean values of three measurements. The error bars indicate standard deviations.

Since PDMS is a kind of silicon rubber, the dependence of E_{PDMS} on temperature (T) has the entropy effect [29]:

$$E_{PDMS} = \frac{\alpha kT}{N\upsilon} \quad (1)$$

where k is the Boltzmann constant, N is the number of monomers between two cross-link points, υ is the molecular volume of a monomer and α is a numerical factor. The rubber counters the stretching action by increasing its chain conformations. A higher temperature increases the conformations and sequentially the entropy. The stretching of rubber at higher temperature is more difficult, thus a larger E is obtained at higher temperatures. According to the theory, E should be linearly proportional to the temperature for a given rubber. However, the entropy–rubbery effect of PDMS (GP) was only found at temperatures larger than T_c (Figs. 2 and S4). Since the increase in conformations of PDMS is mainly due to the rotation of $[Si(CH_3)_2–O]$ bonds [8], a shorter chain between two cross-link points (smaller N) has to overcome a higher energy barrier in order to rotate (increase the conformation). Increasing the temperature over certain value, like T_c, PDMS chain can rotate freely in the 3D network. Therefore, the longer the PDMS chain between two cross-link points is, the lower the T_c will be. In other words, less cross-linked PDMS (less cross-linker or higher c_G) will have a smaller T_c (Figs. 3c, 4c). Once the chain gets enough mobility at a temperature above T_c, E_{PDMS} (E_{GP}) increased rapidly with temperature. From Eq. (1), we know that:

$$\delta_E = \frac{E_{PDMS}}{T} = \frac{\alpha k}{N\upsilon} \quad (2)$$

From Eq. (2), δ_E is inversely proportional to N. Therefore, a higher concentration of graphene in GP (Fig. 3d) or a less amount of cross-linker for PDMS (Fig. 4d) would result in a smaller δ_E.

It is noted that the increase in E_{PDMS} during period II is not reversible. Decreasing temperature to RT resulted in an $E_{PDMS,RT}'$ much larger than $E_{PDMS,RT}$, suggesting that the increase in E_{PDMS} in period II is not only due to the entropy effect, but also due to irreversible chemical reactions. When the chains, especially the dangling chains with one free end, gain enough energy to move freely at a higher temperature (above T_c), further chemical reaction happens [30, 31]. This kind of further chemical reaction only initiates when the temperature is above T_c. Otherwise, the E_{PDMS} remains constant, for instance below 100 °C which is widely chosen as the curing temperature for PDMS (Fig. 5). Three cycles of heating

and cooling under DMA, which means a total test period of ~ 6 h, did not cause obvious change to E_{PDMS}. Similarly, E_{GP} also kept constant during heating/cooling cycles, when the maximum temperature was below T_c (Fig. S6). The explanations are in accordance with the previous reports [10, 11], where the chemical cross-linking was ignored over the physical cross-linking at elevated temperatures, i.e. the temperatures below T_c of PDMS. It therefore confirms that T_c represents the energy barrier inhibiting the free rotation of PDMS chains, which determines the further chemical reaction in cross-linked PDMS, and more importantly, the entropy–rubber properties of PDMS and GP.

Molecular dynamics (MD) simulation was employed to study the interactions between single PDMS chain ($PDMS_c$) and graphene sheet/PDMS network ($PDMS_n$) (Fig. 6). $PDMS_c$ mimics the pendant and unconnected short chains in $PDMS_n$. $PDMS_c$ shows strong affinity with $PDMS_n$ that the interaction energy at RT is − 17.6 kcal mol^{-1} (negative value means attraction), as $PDMS_c$ and $PDMS_n$ have the identical composition (Fig. 6a). The attraction between $PDMS_c$ and $PDMS_n$ reduces as temperature increases. For instance, the interaction energy for $PDMS_c/PDMS_n$ at 200 °C greatly reduced to − 4.4 kcal mol^{-1}. It suggests that pedant chains attached to the networks (or the unconnected short chains with reactive groups) in $PDMS_n$ are bound to the network at RT and are difficult to move around, which greatly reduces the chance for them to meet another reactive moiety. Once these reactive moieties get enough energy to move around (i.e. at a temperature above T_c), further reaction could be re-initiated, causing the further cross-linking of PDMS network.

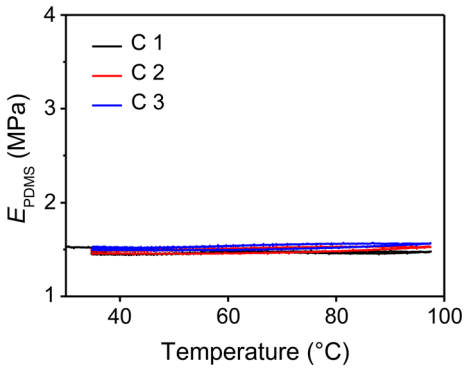

Figure 5 Evolution of elastic modulus of PDMS (E_{PDMS}) during representative heating–cooling cycles (C1–C3) below T_c.

When graphene is added to the system, $PDMS_c$ has an even stronger attraction to graphene (− 25.5 kcal mol^{-1} at RT) than to $PDMS_n$ (Fig. 6a). The large difference in electronegativity between silicon and oxygen atoms in the main chain of PDMS causes the partial ionic nature of the (Si–O) bond [32], which would induce strong interactions between PDMS and graphene. It helps the dispersion of graphene in PDMS precursor and therefore the resulting GP. On the other hand, this strong interaction hinders the rotation of $[Si(CH_3)_2–O]$ bonds in pendant chains, and therefore inhibits the cross-linking of PDMS close to the graphene surface (Fig. 6b). It agrees very well with previous reports that the addition of graphene would inhibit the cross-linking of PDMS [11]. Moreover, the wrinkled structure of graphene (Fig. 1c) may separate the reacting moieties of PDMS from each other, build a physical barrier, and hinder the cross-linking. The inhibited cross-linking was confirmed by the modulus mapping with atomic force microscopy (Fig. 7). The elastic modulus around graphene sheet was greatly reduced as compared to that of the locations slightly away from the graphene sheet. It suggests that graphene only hinders the cross-linking of PDMS close to its surface. Similar to $PDMS_c/PDMS_n$, $PDMS_c$/graphene interaction also gets weaker when the temperature increases. A higher temperature thus increases the chance for $PDMS_c$ close to the graphene surface to get further cross-linking (Fig. 6b). Once the monomers or short chains gain enough mobility at temperature above T_c, further cross-linking could be realized.

While the addition of graphene decreases the E_{PDMS} locally, the large elastic modulus of graphene, which is around 1000 GPa, will certainly increase the apparent elastic modulus of the composite GP [6, 7]. Therefore, the increase in E_{GP} due to the addition of graphene and the decrease in E_{GP} originated from the inhibited cross-linking of PDMS compete with each other: within the concentration range between 0 and 0.4 wt%, the large elastic modulus of graphene and the concentration of grapheme dominate the increment of E_{GP}. A larger amount of graphene (0.4–1.2 wt%) causes less cross-linking of PDMS, which results in a decrease in E_{GP}. It is worth mentioning that, with a much larger c_G in PDMS, the elastic modulus of graphene could once again dominate the E_{GP} as reported in Ref. [6].

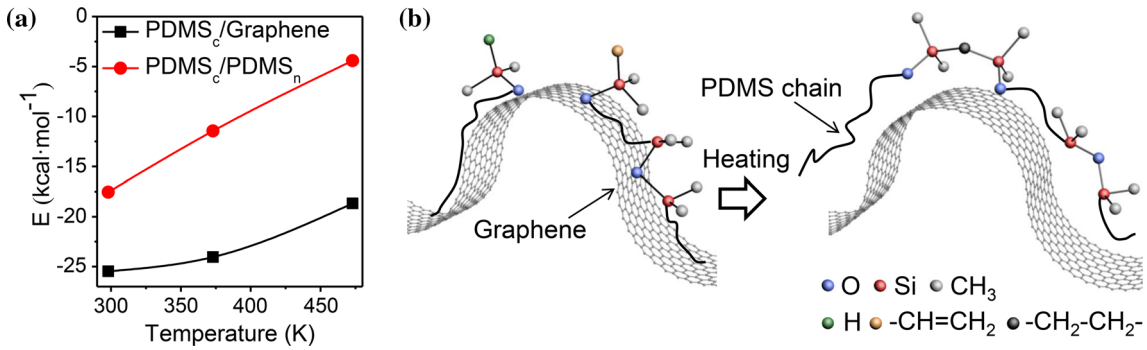

Figure 6 **a** Absolute value of interaction energy E of PDMS$_c$/PDMS$_n$ and PDMS$_c$/graphene at various temperatures. **b** The schematic illustration of the re-initiation of PDMS cross-linking at elevated temperatures.

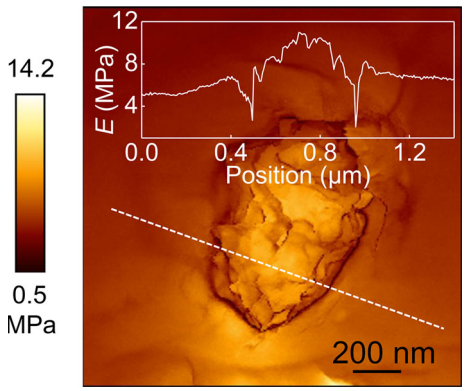

Figure 7 Elastic modulus map around a graphene sheet in GP. The profile of the elastic modulus along the dashed line is shown in the inset.

Conclusions

In this study, the influence of temperature on the elastic modulus of PDMS and PDMS/graphene nanocomposite (GP) was thoroughly investigated. A critical temperature, T_c, was found to govern the temperature dependence of E_{GP} (E_{PDMS}). T_c is dependent on the cross-link degree of PDMS that a larger cross-link degree results in a larger T_c. E_{GP} (E_{PDMS}) is constant when the temperature is below T_c. Above T_c, PDMS chains gain enough energy to move around causing the fast increase in E_{GP} (E_{PDMS}), which is the result of further curing of PDMS and the effect of entropy elasticity. At a higher temperature, E_{GP} (E_{PDMS}) could be twice more than that at room temperature. The addition of graphene retards the cross-linking of PDMS close to its surface and therefore reduces the E_{GP}. The 1.2 wt% of graphene could result in a 43% reduction in E_{GP} at RT. The MD simulation suggested that the strong affinity between pendent chains and PDMS network/graphene sheets hinders the cross-linking of PDMS. Once these chains gain enough energy, in other words overcomes the energy barrier, further cross-linking could be re-initiated. Our results give the hint why the elastic moduli of PDMS in the literature differ quite a lot. Special attention should be paid to the using temperature of PDMS and its composite, especially those could be subjected to a high temperature during application.

Acknowledgements

Authors thank Dr. Rakesh Das for the language editing of this article. The research was funded by National Key R&D Program of China (2018YFB1105100, 2016YFA0200200) and National Natural Science Foundation of China (51503156, 51973165).

Compliance with ethical standards

Conflict of interest The authors declare no conflict of interest.

Electronic supplementary material: The online version of this article (https://doi.org/10.1007/s10853-019-04126-y) contains supplementary material, which is available to authorized users.

References

[1] Jiang W, Niu D, Liu H et al (2014) Photoresponsive soft-robotic platform: biomimetic fabrication and remote actuation. Adv Funct Mater 24:7598–7604

[2] Hu Y, Wu G, Lan T, Zhao J, Liu Y, Chen W (2015) A graphene-based bimorph structure for design of high performance photoactuators. Adv Mater 27:7867–7873

[3] Yan C, Wang J, Lee PS (2015) Stretchable graphene thermistor with tunable thermal index. ACS Nano 9:2130–2137
[4] Zdrojek M, Bomba J, Łapińska A et al (2018) Graphene-based plastic absorber for total sub-terahertz radiation shielding. Nanoscale 10:13426–13431
[5] Boland CS, Khan U, Ryan G et al (2016) Sensitive electromechanical sensors using viscoelastic graphene–polymer nanocomposites. Science 354:1257–1260
[6] Zhang Y, Zhu Y, Lin G, Ruoff RS, Hu N, Schaefer DW, Mark JE (2013) What factors control the mechanical properties of poly(dimethylsiloxane) reinforced with nanosheets of 3-aminopropyltriethoxysilane modified graphene oxide? Polymer 54:3605–3611
[7] Zhao YH, Zhang YF, Bai SL (2016) High thermal conductivity of flexible polymer composites due to synergistic effect of multilayer graphene flakes and graphene foam. Compos Part A Appl Sci Manuf 85:148–155
[8] Wolf MP, Salieb-Beugelaar GB, Hunziker P (2018) PDMS with designer functionalities—properties, modifications strategies, and applications. Prog Polym Sci 83:97–134
[9] Fang M, Zhang Z, Li J, Zhang H, Lu H, Yang Y (2010) Constructing hierarchically structured interphases for strong and tough epoxy nanocomposites by amine-rich graphene surfaces. J Mater Chem 20:9635–9643
[10] Terrones M, Martín O, González M, Pozuelo J, Serrano B, Cabanelas JC, Vega-Díaz SM, Baselga J (2011) Interphases in graphene polymer-based nanocomposites: achievements and challenges. Adv Mater 23:5302–5310
[11] Cao L, Wang Y, Dong P, Vinod S, Tijerina JT, Ajayan PM, Xu Z, Lou J (2016) Interphase induced dynamic self-stiffening in graphene-based polydimethylsiloxane nanocomposites. Small 12:3723–3731
[12] Xue L, Sanz B, Luo A et al (2017) Hybrid surface patterns mimicking the design of the adhesive toe pad of tree frog. ACS Nano 11:9711–9719
[13] Guo Q, Luo Y, Liu J, Zhang X, Lu C (2018) A well-organized graphene nanostructure for versatile strain-sensing application constructed by a covalently bonded graphene/rubber interface. J Mater Chem C6:2139–2214
[14] Jesson DA, Watts JF (2012) The interface and interphase in polymer matrix composites: effect on mechanical properties and methods for identification. Polym Rev 52:321–354
[15] Li Q, Liu C, Lin YH, Liu L, Jiang K, Fan S (2015) Large-strain, multiform movements from designable electrothermal actuators based on large highly anisotropic carbon nanotube sheets. ACS Nano 9:409–418
[16] Wang W, Xiang C, Zhu Q, Zhong W, Li M, Yan K, Wang D (2018) Multistimulus responsive actuator with go and carbon nanotube/pdms bilayer structure for flexible and smart devices. ACS Appl Mater Int 10:27215–27223
[17] Stankovich S, Dikin DA, Dommett GHB et al (2006) Graphene-based composite materials. Nature 442:282–286
[18] Papageorgiou DG, Kinloch IA, Young RJ (2017) Mechanical properties of graphene and graphene-based nanocomposites. Prog Mater Sci 90:75–127
[19] Wu ZS, Ren W, Gao L, Liu B, Jiang C, Cheng HM (2009) Synthesis of high-quality graphene with a pre-determined number of layers. Carbon 47:493–499
[20] Casiraghi C, Hartschuh A, Qian H et al (2009) Raman spectroscopy of graphene edges. Nano Lett 9:1433–1441
[21] Malard LM, Pimenta MA, Dresselhaus G, Dresselhaus MS (2010) Raman spectroscopy in graphene. Phys Rep 473:51–87
[22] Khan U, O'Neill A, Lotya M, De S, Coleman JN (2010) High-concentration solvent exfoliation of graphene. Small 6:864–871
[23] Wang Y, Yang R, Shi Z, Zhang L, Shi D, Wang E, Zhang G (2011) Super-elastic graphene ripples for flexible strain sensors. ACS Nano 5:3645–3650
[24] Camino G, Lomakin SM, Lazzari M (2001) Polydimethylsiloxane thermal degradation. Part 1. Kinetic aspects. Polymer 42:2395–2402
[25] Zhang W, Srivastava I, Zhu YF, Picu CR, Koratkar NA (2009) Heterogeneity in epoxy nanocomposites initiates crazing: significant improvements in fatigue resistance and toughening. Small 5:1403–1407
[26] Rafiee MA, Rafiee J, Srivastava I, Wang Z, Song H, Yu ZZ, Koratkar N (2010) Fracture and fatigue in graphene nanocomposites. Small 6:179–183
[27] Asi O (2008) Mechanical properties of glass–fiber reinforced epoxy composites filled with Al_2O_3 particles. J Reinf Plast Compos 28:2861–2867
[28] Liang J, Huang Y, Zhang L, Wang Y, Ma Y, Guo T, Chen Y (2009) Molecular-level dispersion of graphene into poly(vinyl alcohol) and effective reinforcement of their nanocomposites. Adv Funct Mater 19:2297–2302
[29] Doi M, Edwards SF (1986) The theory of polymer dynamics. Oxford University Press, New York
[30] Mark JE (2004) Some interesting things about polysiloxanes. Acc Chem Res 37:946–953
[31] Xue L, Pham JT, Iturri J, del Campo A (2016) Stick–slip friction of PDMS surfaces for bioinspired adhesives. Langmuir 32:2428–2435
[32] Yilgör E, Yilgör I (2014) Silicone containing copolymers: synthesis, properties and applications. Prog Polym Sci 39:1165–1195